

Asymptotic evolution of stimulated Brillouin scattering: Implications for optical fibers

Jean Coste and Carlos Montes

Groupement de Recherches Coordonées (GRECO), Interaction Laser-Matière du Centre National de la Recherche Scientifique, Laboratoire de Physique de la Matière Condensée, Université de Nice, Parc Valrose, 06034 Nice Cédex, France and Observatoire de Nice, Boîte Postale No. 139, 06003 Nice Cédex, France

(Received 28 January 1986)

We consider the nonlinear three-wave stimulated Brillouin scattering where an initial electromagnetic wave packet grows backward in the expense of a constant input pump wave. For long interaction times we show in particular that the backscattered wave envelope exhibits a set of large peaks of decreasing amplitude, the intensity of the first one growing as t^2 while its width shrinks as $1/t$. Moreover, the sound-wave amplitude saturates. In the limit case of strong damping of the sound wave the asymptotic behavior is quite different. Implications of these results are considered concerning the observed mechanical fracture of an optical fiber supporting a large laser pulse.

I. INTRODUCTION

Several nonlinear mechanisms are candidates for limiting the intensity of an electromagnetic pulse propagating along an optical fiber. One of the most important is stimulated Brillouin scattering (SBS) generated by the coupling of the electromagnetic (e.m.) wave with the thermal acoustic fluctuations of the fiber. Various experimental and theoretical studies have been devoted to SBS in single-mode optical fibers,^{1,2} and also in laser plasma devices, mainly in order to avoid it.³ This process is indeed so efficient that it has been conjectured in the pioneering paper of Kroll⁴ that it could cause the mechanical fracture of the optical material. But such phenomenon would occur at very large e.m. intensities which make the dynamics strongly nonlinear, and up to now not well understood. However results on the nonlinear dynamics are crucial in order to determine at which flux intensity catastrophic effects such as a mechanical fracture are expected. Interesting results concerning this problem have recently obtained⁵ by numerical integration of the equations associated with SBS which show the complex structure of the backward wave envelope at large time. We present here analytical and numerical results which yield the asymptotic time evolution of the amplitude and the shape of the three wave envelopes. We give an order of magnitude of the radiation pressure of the backward wave in a typical optical-fiber experiment, and we compare it with the fracture pressure of the material. We also suggest that another contributing mechanism could be the nonlinear propagation of the initial constraints generated by the e.m. pulse, after its passage. We finally emphasize that we consider the pure three-wave problem; in particular no thermal fluctuations are taken into account and therefore multiple scattering is absent in this model.

II. ENVELOPE MODEL

In the simplest version of SBS, two quasimonochromatic waves $E_1 \exp[i(\omega_1 t - \mathbf{k}_1 \cdot \mathbf{x})]$, the pump, and

$E_2 \exp[i(\omega_2 t + \mathbf{k}_2 \cdot \mathbf{x})]$, the backward scattered wave, are propagating in opposite directions and couple with a forward acoustic wave $E_s \exp[i(\omega_s t - \mathbf{k}_s \cdot \mathbf{x})]$. (For convenience we describe the acoustic wave by means of a variable E_s which has the dimension of an electric field and which is proportional to the acoustic density ρ_s .) The frequencies and wave vectors ω_i and $k_i = |\mathbf{k}_i|$ obey the conservation laws of the resonant interaction:

$$\omega_s = \omega_1 - \omega_2 ,$$

$$k_s = k_1 + k_2 .$$

Assuming the waves to be quasimonochromatic is equivalent to saying that the spatial extension of the three wave packets is large and therefore that a description of the interaction in terms of slowly varying complex amplitudes $E_i(x, t)$ is available. Finally we assume, as usual in monomode fibers, that a plane-wave approximation is justified. Then the problem is one dimensional in space and the E_i obey the following equations:

$$\begin{aligned} (\partial_t + \partial_x)E_1 &= -KE_2E_s , \\ (\partial_t - \partial_x)E_2 &= KE_1E_s^* , \\ (\partial_t + \varepsilon\partial_x + \gamma)E_s &= KE_1E_2^* . \end{aligned} \quad (1)$$

K is the SBS coupling constant and γ is the damping rate of the acoustic wave. We neglect the damping of e.m. waves. The velocity of light is made equal to unity, and $\varepsilon = c_s/c$ is the ratio of sound to light velocity. We rewrite Eqs. (1) in dimensionless form after introducing time and length scales $T = 1/KE_p$ and $L = T$, E_p being the initial amplitude of pump E_1 , and measuring the fields in units of E_p . We obtain

$$\begin{aligned} (\partial_t + \partial_x)E_1 &= -E_2E_s , \\ (\partial_t - \partial_x)E_2 &= E_1E_s^* , \\ (\partial_t + \varepsilon\partial_x + \mu)E_s &= E_1E_2^* , \end{aligned} \quad (2)$$

where $\mu = \gamma T = 2\varepsilon\rho\omega_1 T$, $\rho = \gamma/\omega_s$ being the relative damping rate of the sound wave. The dynamical equations depend on parameters ε and μ , and it is important to

note that, in a typical experiment of nonlinear propagation with moderate pump energy (say of the order of 1 mW), μ may be larger than unity, even though ρ is small (say $\rho \sim 10^{-3}$). In this case the SBS coupling is indeed resonant ($\rho \ll 1$) as it should be in the envelope approximation; nevertheless the dynamics is *a priori* of the "strongly damped" type since the damping time of the sound wave is smaller than the characteristic time T of the nonlinear evolution.

III. STRONGLY DAMPED CASE

The strongly damped case corresponds to the limit $\mu \gg 1$. Then E_s will follow adiabatically the excitation of fields E_1 and E_2 . This means that E_s will be replaced in Eqs. (2) by

$$E_s = E_1 E_2^* / \mu,$$

which gives

$$\begin{aligned} (\partial_t + \partial_x) I_1 &= -I_1 I_2, \\ (\partial_t - \partial_x) I_2 &= I_1 I_2, \end{aligned} \quad (3)$$

where $I_j = |E_j|^2$. In Eqs. (3) we use a new time scale, namely $T' = \mu T / 2 = \epsilon \rho \omega_1 T^2$. These equations are well known and are for instance used in the context of SBS in fibers by Bar-Joseph *et al.*⁶ for studying relaxation oscillations.

Fortunately there exists an exact solution of Eqs. (3), obtained in 1977 by Chu and Karney.⁷ We shall use it for analyzing the asymptotic evolution of a system corresponding to the initial condition as found in Fig. 1. The supports of the initial profiles $I_1(x, 0)$ and $I_2(x, 0)$ are disjoint. $I_2(x, 0)$ has a finite extension while $I_1(x, 0)$ extends to infinity toward the left with constant amplitude. In other words we study the interaction of a finite packet of backward waves with a pump of infinite spatial extension.

Let us put $I_1(x, 0) = P_1(x)$ and $I_2(x, 0) = P_2(x)$. The general solution of the initial-value problem is

$$I_1(x, t) = [Z(\xi) - T(\tau)]^{-1} (\partial_t - \partial_x) T(\tau), \quad (4)$$

$$I_2(x, t) = [Z(\xi) - T(\tau)]^{-1} (\partial_t + \partial_x) Z(\xi), \quad (5)$$

where $\xi = (t + x)/2$, $\tau = (t - x)/2$, and

$$\begin{aligned} 2Z(\xi) &= 1 + \int_0^{2\xi} dy P_2(y) \exp \left[\int_0^y [P_1(z) + P_2(z)] dz / 2 \right], \\ 2T(\tau) &= -1 - \int_0^{-2\tau} dy P_1(y) \exp \left[\int_0^y [P_1(z) + P_2(z)] dz / 2 \right]. \end{aligned}$$

For initial disjoint supports, the above expressions reduce to

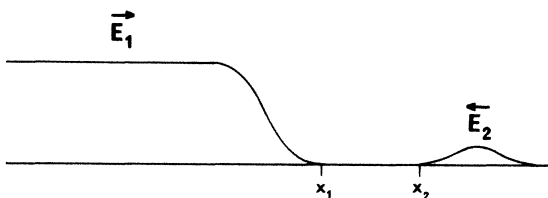


FIG. 1. Shape of the initial envelopes $E_1(x, 0)$ and $E_2(x, 0)$.

$$\begin{aligned} Z(\xi) &= -\frac{1}{2} + \exp \left[\int_0^{2\xi} P_2(y) dy / 2 \right] \\ &= -\frac{1}{2} + \exp \left[\int_{x_2}^{2\xi} P_2(y) dy / 2 \right], \\ T(\tau) &= \frac{1}{2} - \exp \left[\int_0^{-2\tau} P_2(y) dy / 2 \right] \\ &= \frac{1}{2} - \exp \left[\int_{x_1}^{-2\tau} P_2(y) dy / 2 \right], \end{aligned}$$

x_1 and x_2 being, respectively, the upper and lower bound of P_1 and P_2 .

We shall now show that the asymptotic profile $I_2(x, t)$ is extremely peaked in the vicinity of the left bound $x_2(t) = x_2 - t$ of the wave packet at time t . Let us put $x = x_2 - t + \eta$ and

$$\begin{aligned} A &= \int_{x_1}^{-2\tau} P_2(y) dy / 2 \\ &= \int_{x_1}^{x_2 + \eta - 2t} P_2(y) dy / 2 \rightarrow -t P_1(-\infty) \text{ at large } t, \\ B &= \int_{x_2}^{2\xi} P_2(y) dy / 2 = \int_{x_2}^{x_2 + \eta} P_2(y) dy / 2. \end{aligned}$$

[A and B are the integrals entering above expressions for $Z(\xi)$ and $T(\tau)$.] For $P_1(-\infty) = 1$ (intensity of the pump normalized to unity), $A(t \rightarrow -\infty) \simeq -t$. Concerning B , it is determined, for small η , by the analytic behavior of P_2 in the neighborhood of x_2 . Let $P_2 \simeq \alpha(x - x_2)^n$, we obtain $B \simeq \alpha \eta^{n+1} / (n+1)$. From expression (5) we obtain, in the limit of large t ,

$$I_2 = \alpha \eta^n \{ e^{-t} + \alpha \eta^{n+1} / [2(n+1)] \}^{-1}. \quad (6)$$

This function is maximum at

$$\eta = \delta = [2n(n+1)/\alpha]^{1/(n+1)} e^{-t/(n+1)},$$

at which value

$$I_2 = I_{2\max} = 2(n^{n/(n+1)}) \{ \alpha / [2(n+1)] \}^{1/n} e^{t/n},$$

and the width of the peak is of the order of δ .

We see that the backward wave packet is extremely peaked and that its amplitude grows and its width shrinks exponentially in time. Therefore this very simple model exhibits the striking property of the unlimited compression of the I_2 profile. Let us remark that the asymptotic behavior is completely determined by the analytic properties of the initial profile P_2 in the vicinity of the lower bound of its support. Such a behavior is obviously singular, and it may be shown that it does not survive if P_2 's support is not left bounded. As an example, if P_2 is Gaussian, then we found that I_2 grows only as \sqrt{t} . These results show that the adiabatic model fails at large time: Indeed when the width of the I_2 's peak becomes overly small, the characteristic time of evolution becomes smaller than the damping time of the sound wave. We are therefore led to study the general case of a finite damping.

IV. GENERAL CASE

The mathematical problem in the three-waves general case is much more complex. Let us observe that, in the limit $\mu \rightarrow 0$, it reduces to the coupling of three undamped waves, and the equations are formally integrable by the

method of inverse scattering. However, in the present case where one of the waves is of the acoustic type, the sign of the coupling coefficient is such that no solitonic solution (i.e., corresponding to a discrete eigenvalue of the associated spectral problem) is available.⁸ Then the existence of a formal solution is probably not of great help. Therefore we have primarily made a numerical investigation. It proves useful to introduce the variable change ($x \rightarrow x + t; t \rightarrow t$) into Eqs. (2). In terms of these new variables these equations read:

$$\begin{aligned} \partial_t E_2 &= E_1 E_s^* , \\ (\partial_t + 2\partial_x) E_1 &= -E_2 E_s , \\ [\partial_t + (1 + \epsilon)\partial_x + \mu] E_s &= E_1 E_2^* . \end{aligned} \tag{7}$$

We are dealing with the same type of initial value problem as in the preceding section. In addition we assume that the support of $E_s(x,0)=0$. Again we assume that the support of $E_2(x,0)$ has a lower bound ($x=0$), and that $E_2(0,0)=0$. Then it can be shown that the initial value problem on \mathbb{R} is equivalent to a problem on $\mathbb{R}_+(0, +\infty)$, provided we add boundary values $E_1(0,t)=1$ and $E_s(0,t)=0$. The validity of this statement relies upon the vanishing of E_2 and E_s at the origin. This initial-boundary-value problem is more suitable for numerical integration. Now we observe that ϵ in a fiber is very small ($\epsilon \sim 10^{-5}$), and it appears in Eqs. (7) only as a slight modification of the relative velocity of the sound wave. Therefore one may conjecture that to take into account a nonzero c_s has only a small effect on the asymptotic behavior of the solutions. This will be later confirmed. Another remark is the following. It may be shown (see Appendix A) that, with the above boundary conditions, the relative phases φ_i of the complex amplitudes E_i are time independent, except for sudden π shifts which appear when the fields vanish (i.e., these shifts are simply associated with the change of sign of the fields when they cross value zero). An obvious consequence is that the φ_i stay also x independent as they were at initial time. Then it is easily seen that Eqs. (7) reduce (with the help of an appropriate scaling) to

$$\begin{aligned} \partial_t Y_2 &= Y_1 Y_s , \\ (\partial_t + 2\partial_x) Y_1 &= -Y_2 Y_s , \\ [\partial_t + (1 + \epsilon)\partial_x + \mu] Y_s &= Y_1 Y_2 , \end{aligned} \tag{8}$$

where the Y_i are the real part of the complex fields E_i ; i.e., $Y_i \equiv \text{Re} E_i \equiv E'_i$. In the limiting case $\epsilon=0$, we have elaborate a convenient Runge-Kutta algorithm (see Appendix B) for solving Eqs. (8). This algorithm appears quite stable and fast and it has provided the profiles plotted on Figs. 2–4.

Our results reproduce the complex structure of the backward wave profile observed by Damzen and Hutchinson⁵ with successive π phase shifts of E'_1 and E'_2 . As in the strongly damped model we observe the remarkable unlimited compression of the first E'_2 peak and its shift toward the front edge of the backward pulse. These results suggest the same remark as in the preceding section, namely: at large times, the dynamics of the first peak be-

comes dissipationless. Moreover the observed time variation of the amplitudes (see Fig. 5) and of the profiles shape suggest asymptotic scale laws.

Let us look for an asymptotic solution of the form:

$$\begin{aligned} Y_1(x,t) &= f_1(\xi) , \\ Y_2(x,t) &= t^\alpha f_2(\xi) , \\ Y_s(x,t) &= t^\beta f_s(\xi) , \end{aligned} \tag{9}$$

where $\xi = xt^\nu$. Making the change of variable $x \rightarrow \xi, t \rightarrow t$, we have

$$\begin{aligned} \partial_t &\rightarrow \partial_t + \nu(\xi/t)\partial_\xi , \\ \partial_x &\rightarrow \xi t^\nu \partial_\xi . \end{aligned}$$

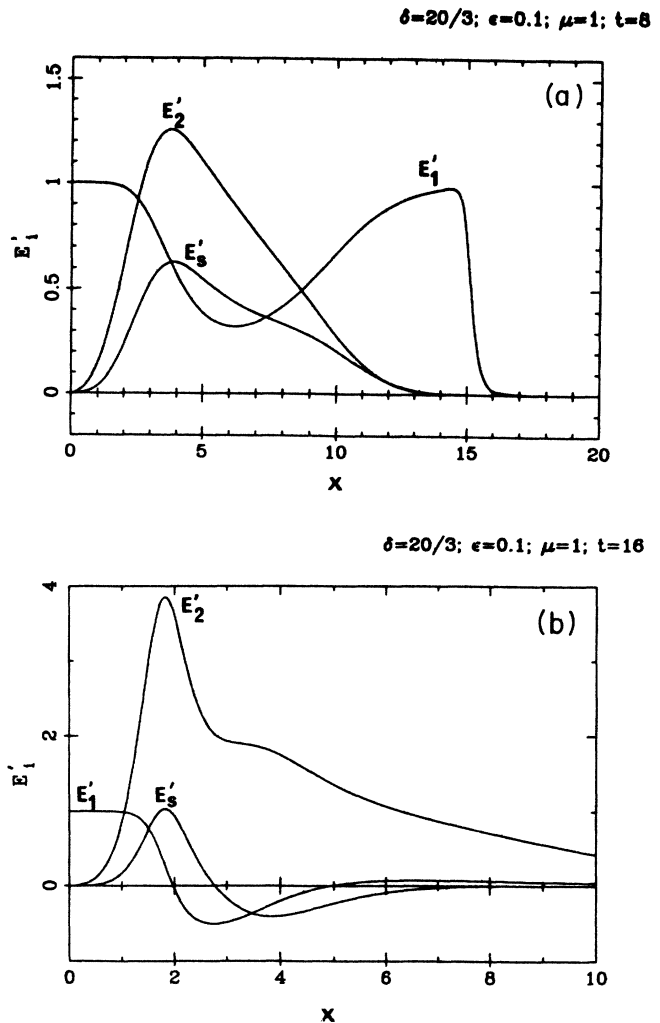


FIG. 2. (a) Three-wave envelopes for $E'_i = \text{Re} E_i = Y_i$ in the reference frame of backward wave E'_2 : transient stage at $t=8$. Dimensionless units: $E'_i \rightarrow E'_i/E'_p$; $t \rightarrow t/T = tKE'_p$; $x \rightarrow x/L = KE'_p/c$; $\mu = \gamma T = 2\epsilon\rho\omega_1 T = \gamma/(KE'_p) = 1$. Boundary-initial conditions: $E'_1(0,t)=1$; $E'_2(0,t)=E'_s(0,t)=0$. Initial profile for $E'_2(x,0)$: amplitude $\epsilon=0.1$; width $\delta = \frac{20}{3}$. The figure shows the initial depletion of the pump E'_1 . (b) Same as (a) at time $t=16$. A second E'_2 peak appears, while E'_1 changes its sign: phase reversal of the pump field (“ π pulse”).

Replacing in Eqs. (8) the Y_i by expressions (9), we obtain

$$t^{\alpha-1}(\alpha f_2 + v\xi \partial_\xi f_2) = t^\beta f_1 f_s, \quad (10)$$

$$v(\xi/t) \partial_\xi f_1 + 2t^\nu \partial_\xi f_1 = -t^{\alpha+\beta} f_2 f_s, \quad (11)$$

$$[\mu t^\beta + t^{\beta-1}(\beta + v\xi \partial_\xi)] f_s + (1 + \varepsilon) t^{\nu+\beta} \partial_\xi f_s = t^\alpha f_1 f_2. \quad (12)$$

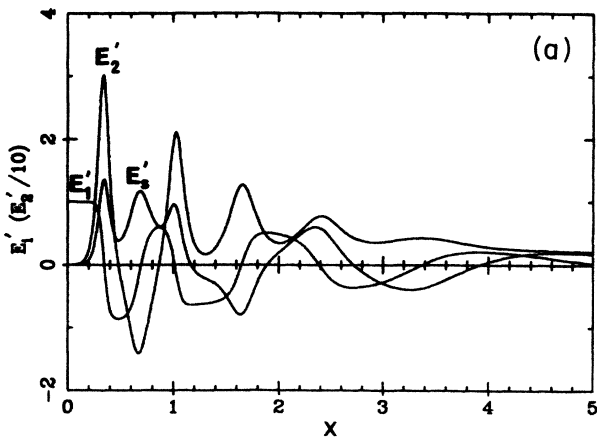
Now the idea of our asymptotic expansion is to look for a solution of form (9), with finite f_i , in the limit $t \rightarrow \infty$. From numerical results we infer that $\nu \approx 1$ and $\beta < 1$. This leads us to neglect the first left-hand-side terms of Eqs. (11) and (12) as being small compared to the second ones. Then Eqs. (10), (11), and (12) can be put in the form

$$(\alpha + v\xi \partial_\xi) f_2 / (f_1 f_s) = t^{\beta+1-\alpha},$$

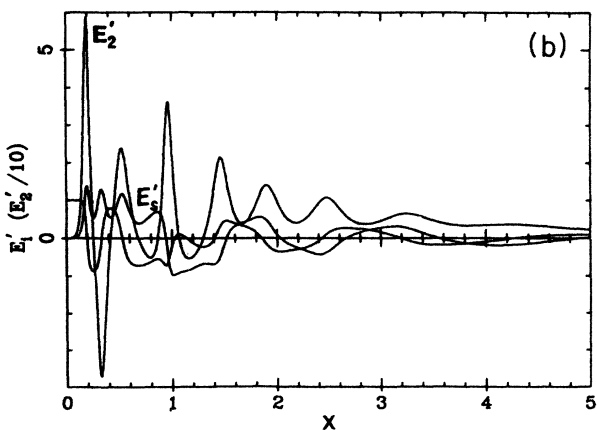
$$2 \partial_\xi f_1 / (f_2 f_s) = -t^{\alpha+\beta-\nu},$$

$$(1 + \varepsilon) \partial_\xi f_s / (f_1 f_2) = t^{\alpha-\beta-\nu}.$$

$\delta=20/3; \varepsilon=0.1; \mu=1; t=136$



$\delta=20/3; \varepsilon=0.1; \mu=1; t=288$



The compatibility condition of these equations is obviously $\alpha=1, \beta=0$, and $\nu=1$. Therefore the asymptotic solutions are of the form:

$$Y_1(x,t) = f_1(\xi),$$

$$Y_2(x,t) = t f_2(\xi),$$

$$Y_s(x,t) = f_s(\xi),$$

(13)

$\varepsilon=0.1; \mu=1; t_0=136; t_m=280; \Delta t=16$

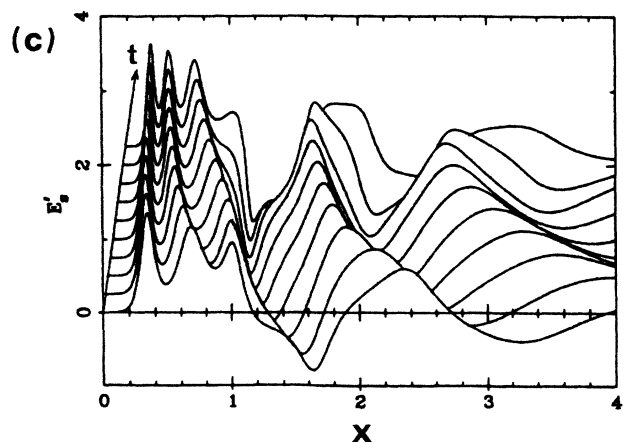
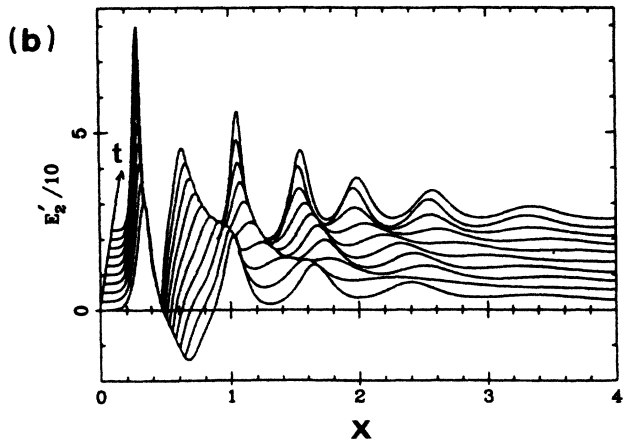
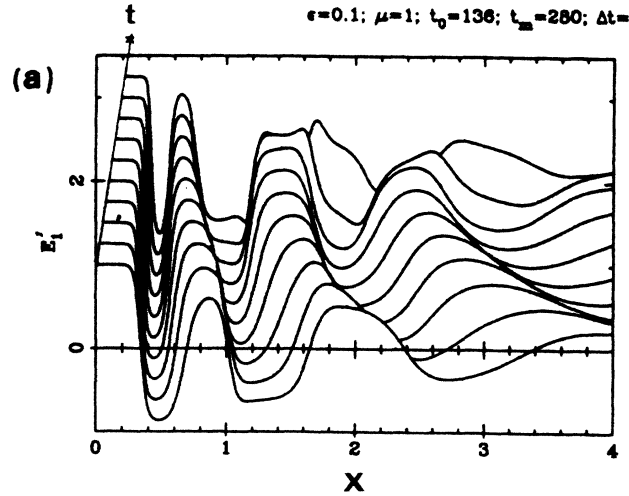


FIG. 3. Steps in the asymptotic time evolution (note that a different scale has been used for E'_2). (a) $t=136$; an opposite π pulse appears in E'_2 profile. Note that E'_2 and E'_s amplitudes slowly decrease as a result of dissipation. (b) $t=288$; the figure shows the complex structure of the envelopes.

FIG. 4. Space-time evolution of the envelopes for $136 < t < 288$. (a) E'_1 pump wave envelope. (b) E'_2 backscattered wave envelope (scale is $\frac{1}{10}$). (c) E'_s acoustic wave envelope.

where $\xi = xt$, the f_i 's obeying the system of ordinary differential equations:

$$f_2 + \xi df_2/d\xi = f_1 f_s, \tag{14}$$

$$2df_1/d\xi = -f_2 f_s, \tag{15}$$

$$(1 + \epsilon)df_s/d\xi = f_1 f_2. \tag{16}$$

The general solution of Eqs. (14)–(16) depend upon three parameters A_i , some of which could *a priori* be determined by boundary conditions at $\xi = 0$, namely $f_1(0) = 1$ and $f_2(0) = f_s(0) = 0$. Here we encounter a difficulty. Condition $f_2(0) = 0$ must be shown impossible to satisfy, except for the trivial solution $f_2(\xi) = 0$. Indeed the solution of Eqs. (14)–(16) must reduce at small ξ to the solution of linearized Eqs. (14) and (16), where f_1 has been replaced by unity. These equations yield the following equation for f_2 :

$$\xi f_2'' + 2f_2' = f_2, \tag{17}$$

whose general solution is of the form

$$f_2 = \xi^{-1/2} [AJ_1(2i\sqrt{\xi}) + BN_1(2i\sqrt{\xi})], \tag{18}$$

J_1 and N_1 being the usual Bessel and Neumann functions, and A and B arbitrary constants. $f_2(0)$ is either infinite ($B \neq 0$) or equal to A ($B = 0$).

We conclude that, if there exists a particular solution of Eqs. (14)–(16)—let us call it in vector form Y^{II} —which is an approximate asymptotic solution of the partial differential equation (PDE) Eqs. (8), its support must not include some neighborhood of the origin. This statement can be made more precise by considering the solution of linearized Eqs. (8) around $Y_1 = 1$, namely:

$$\partial_t Y_2 = Y_s, \tag{19}$$

$$[\partial_t + (1 + \epsilon)\partial_x + \mu] Y_s = Y_2. \tag{20}$$

We show in Appendix C that, for an initial condition of the form

$$Y_2(x, 0) \simeq x^n \text{ (for small } x \text{)},$$

the asymptotic solution of Eqs. (19) and (20) is

$$Y_2(x, t) \simeq t^{-n} \xi^n J_n(2i\sqrt{\xi}), \tag{21}$$

$$Y_s(x, t) \simeq t^{-(n+1)} \xi^n [(1-n)J_n(2i\sqrt{\xi}) - 2i\xi J_n'(2i\sqrt{\xi})], \tag{22}$$

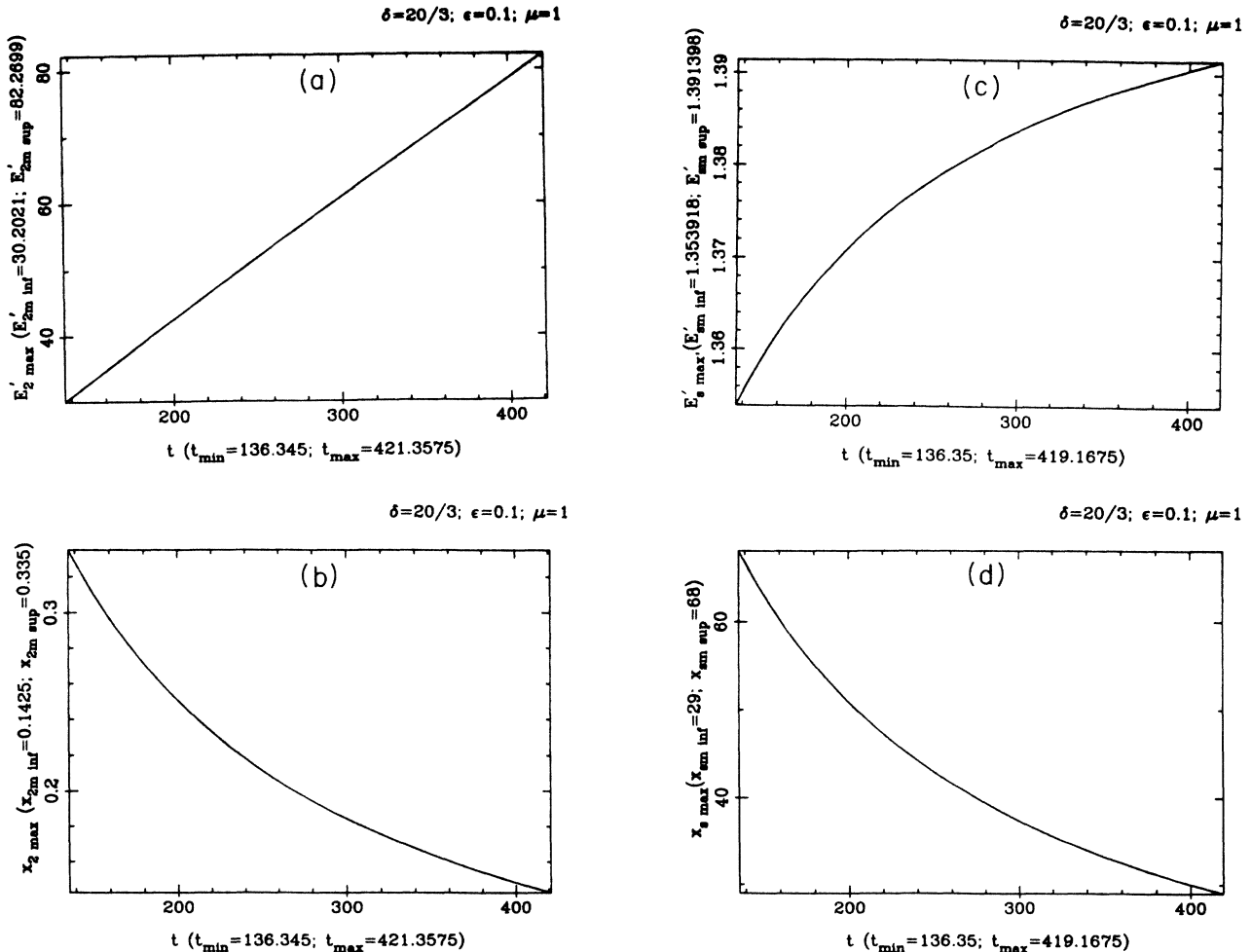


FIG. 5. Asymptotic time evolution of: (a) Amplitude of E_2' first peak ($E_2'_{\text{max}}$). (b) Distance of this peak from the front's edge ($x_{2\text{max}}$). (c) and (d) same but for E_s' . (Subscripts inf and sup delimit the ordinate interval, and min and max the time interval.)

where $\xi = xt/(1+\varepsilon)$. Let us call Y^I this solution [$Y^I = (Y_1, Y_2, Y_s)$] with $Y_1(x, t) = 1$. The domain of validity of Y^I is roughly defined by the condition that the product $Y_2 Y_s$ is much smaller than unity. This gives, by using the asymptotic evaluation of the Bessel functions: $\xi \ll \xi^* = (n \log t)^2$. As a result, the lower bound of Y^{II} support, being of the order of ξ^* , is not small [remember of course that $x^* = (1+\varepsilon)\xi^*/t$ is very small: therefore the excluded domain in x space is vanishingly small at large t]. Y^I and Y^{II} should be linked through the exact solution of the nonlinear PDE which in some neighborhood of ξ^* is neither of type Y^I nor of type Y^{II} [see Fig. 6(b)].

Since ξ^* is a (logarithmic) slowly varying function of time, we may conjecture that there exists a perturbative analysis of the exact solution based on separate time scales, in which Y^{II} would be a slowly varying function of

time through the parameters defining the general solution of Eqs. (14)–(16). A first parameter can be associated with the integral of motion resulting from Eqs. (15) and (16):

$$f_1^2 + [(1+\varepsilon)/2]f_s^2 = K. \quad (23)$$

Making the integration constant equal to unity means that K keeps the same value in domains I and II. This choice is indeed supported by the results of numerical integration of Eqs. (8) (we have observed that K is a weakly oscillating function of ξ whose amplitude is a decreasing function of time). We are then left with a two-parameter family of solutions of Eqs. (14)–(16). An additional requirement could be that Y^{II} does not diverge at the origin, which would indeed determine another parameter [cf. Eq. (18)]. But this argument is not tenable since ξ^* is not small; therefore the fit of Y^{II} with numerical solution Y of the PDE at a given time has been done by taking $K=1$ and by fitting the values of Y_2^{II} and Y_s^{II} with the corresponding components of Y at some ξ arbitrarily chosen in domain II. Before proceeding to the comparison between Y^{II} and Y , the following remark is in order. As was told before we expect, in the case $\mu \neq 0$, Y^{II} to be a good approximation only for sufficiently small x , and in particular in the neighborhood of the first peak. On the contrary the domain of validity of Y^{II} may be much larger when $\mu=0$. Indeed no damping of the acoustic field is to be taken into account, and this corresponds to the fact that in Eqs. (11) and (12) we only have to neglect ξ/t compared to t in the factor multiplying differential operator ∂_ξ . On the contrary, for $\mu \neq 0$, we have to take into account the term μf_s in Eq. (12).

A last question concerns the overall effect of SBS interaction. Is the interaction zone finite? In other words, does E_1 vanish at large distances from the E_2 front, and what happens to E_s ? We have already seen that, in the limit of infinite damping of the acoustic wave, a total reflection of the backward wave is achieved. No obvious answer is available in the general case of finite damping but it can be given in the limit $\mu \rightarrow 0$ provided Y^{II} is actually a good approximation of the asymptotic solution: let us introduce in Eqs. (14)–(16) and (23) written for $K=1$ the change of variables:

$$f_1 = \sin(\theta/2), \quad (24)$$

$$f_s = \sqrt{2} \cos(\theta/2). \quad (25)$$

We then obtain

$$\sqrt{2}f_2 = -\theta', \quad (26)$$

$$\xi\theta'' + \theta' + \sin\theta = 0. \quad (27)$$

It is interesting to point out that Eq. (27), for $\theta \rightarrow \theta + \pi$, has been used by Lamb, Jr. for describing the propagation of a π pulse in a lossless amplifier,⁹ and is connected with a model for the treatment of ultrashort optical pulse propagation.¹⁰ Moreover Eq. (27) can also be derived from the sine-Gordon equation by looking for a self-similar solution of the variable $\xi = (x+t)(x-t)$.¹¹ We show in Ap-

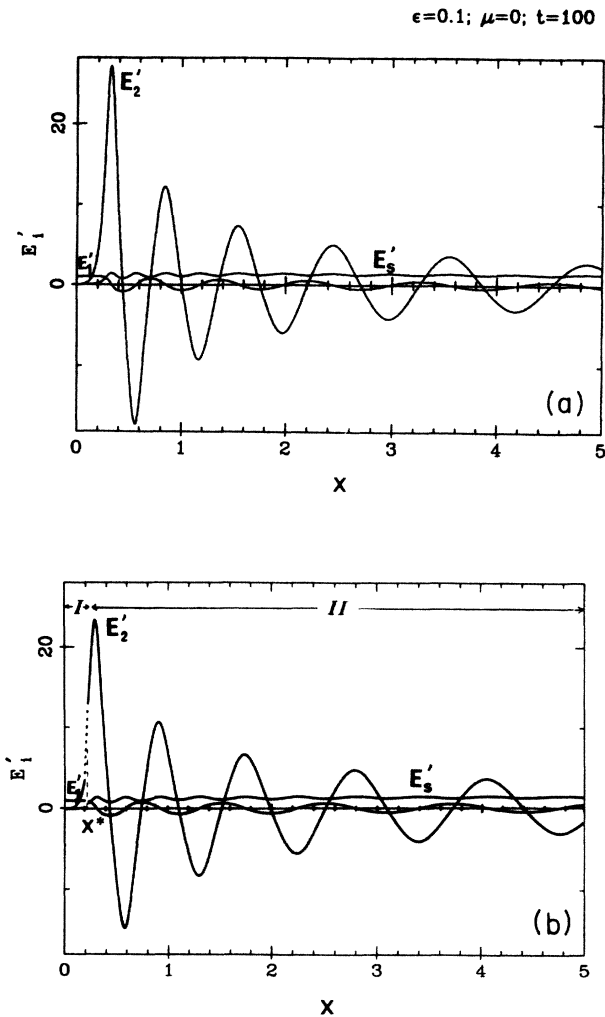


FIG. 6. Comparison of the numerical solutions of PDE (8), (a) with the solutions of the ordinary differential equations (14)–(16) with invariant $K=1$ [cf. Eq. (23)], (b) in the case $\mu=0$. (a) Solution of the PDE at $t=100$. (b) Solution of Eqs. (14)–(16), with integration constants chosen in order to fit E_1' values at the first zero of E_2' . The transient solutions around $x^* = [\log(t)]^2/t$ linking Y^I and Y^{II} are plotted in dotted lines.

pendix D that solutions of Eq. (27) vanish when $\xi \rightarrow \infty$. Then asymptotic solution of linearized Eq. (27) around $\theta=0$ is

$$\begin{aligned} Y_1 &\simeq \theta \simeq \xi^{-1/4} \sin(2\sqrt{\xi} + \phi) \quad (\phi \text{ arbitrary constant}), \\ Y_2 &\simeq t \xi^{-3/4} \sin(2\sqrt{\xi} + \phi), \\ Y_s &\simeq \sqrt{2}. \end{aligned}$$

Let us also observe that a consequence of Eqs. (14)–(16) with $K=1$ is that the maximum value of Y_s is $\sqrt{2}$, a property which is remarkably well verified by numerical integration of the PDE, on the successive maxima of Y_s . We see on the above formulas that the overall spatial extension of the backward field grows like $t^{1/3}$ while Y_1 amplitude decreases as $(xt)^{-1/4}$. This shows that the pump's tail is large, but the reflection coefficient goes to unity at large time.

Equations (14)–(16) have been integrated numerically and their solution (for $\varepsilon=0$) is compared in Figs. 7 with the numerical solution of Eqs. (8) for a long time ($t=288$). The agreement is quite satisfactory as far as the first peak region is concerned for $\mu=1$. In the limiting case $\mu=0$ the agreement is still better, and the domain of validity of Y^{II} larger, as expected; however a deviation is

observed between the spatial period of the oscillations in Y^{II} and Y (see Figs. 6). It is difficult to say if this deviation would disappear at larger times, or if it belongs to the asymptotic state (and then would be obtained in a convenient separate time-scale analysis).

Summarizing the above results on asymptotic behavior, we have shown that:

- (1) The backward wave profile begins with a peak of very large amplitude followed by several secondary peaks.
- (2) The amplitude of the first peak in the asymptotic regime grows as t (the intensity as t^2), and its width shrinks as $1/t$. These two facts are obvious consequences of the scaling law.
- (3) The intensity of the sound wave saturates at twice the value of the pump intensity (in our system of units).
- (4) The existence of the scaling laws seems to confirm the conjecture that the dynamics of the first peak is insensitive to dissipation.
- (5) In the limit $\mu \rightarrow 0$ the nonlinear reflection of the pump wave is total.

We also emphasize that the above results are restricted to the validity of the three-wave envelope model. This obviously gives a lower bound of the peaks' width of the backward wave profile.

V. MECHANICAL EFFECTS ON THE FIBER

Can we expect from the above results a mechanical effect of the backward wave packets on the fiber? At first sight we could guess that the sound wave's pressure could be responsible for that. Let us put some numbers in the theory.

(1) The *proportionality coefficient* $\alpha = \rho_s / E_s$ between E_s and acoustic density fluctuation ρ_s , is given by

$$\alpha = [k_1 / (ck_2)]^{1/2},$$

where

$$k_2 = \pi n^3 p_{12} / (\lambda \rho_0), \quad k_1 = k_2 \rho_0 n^2 \varepsilon_0 / (2c_s).$$

Using Cotter's notations,¹ ρ_0 is the unperturbed fiber density, ε_0 the vacuum dielectric constant, n the refractive index, λ the laser wavelength, and p_{12} the elasto-optic coefficient. With the numerical values of the Cotter's article¹ we find $\alpha \simeq 10^{-10}$ (for $\lambda = 155 \mu\text{m}$, $\gamma / \omega_s \simeq 10^{-3}$).

(2) The *SBS coupling constant* is $K = k_1 / \alpha$. We find $K \simeq 25$. For a fiber's effective cross section of $6 \times 10^{-11} \text{m}^2$, we find that the amplitude E_p of the pump field is $E_p \simeq 10^7 \text{V/m}$ for a laser with power equal to 10W , and that $\mu = 0.2$.

With these numerical values we find for the pressure's amplitude of the sound wave: $p_s \simeq c_s^2 \rho_s \simeq c_s^2 \alpha E_p$, since we have seen that E_s remains smaller than $\sqrt{2} E_p$. This gives $p_s \simeq 0.3 \text{ bars}$. Such a value has to be compared to a relevant elastic coefficient of the fiber, namely the Young modulus, or more accurately to the fracture pressure p_f of the material. A typical value is $p_f \simeq 500 \text{ bars}$. We therefore conclude that the sound pressure generated by resonant SBS interaction cannot produce any appreciable mechanical effect on the fiber. We are then led to consider the effect of the radiation pressure of the backward wave, which is a static pressure. Considering the same

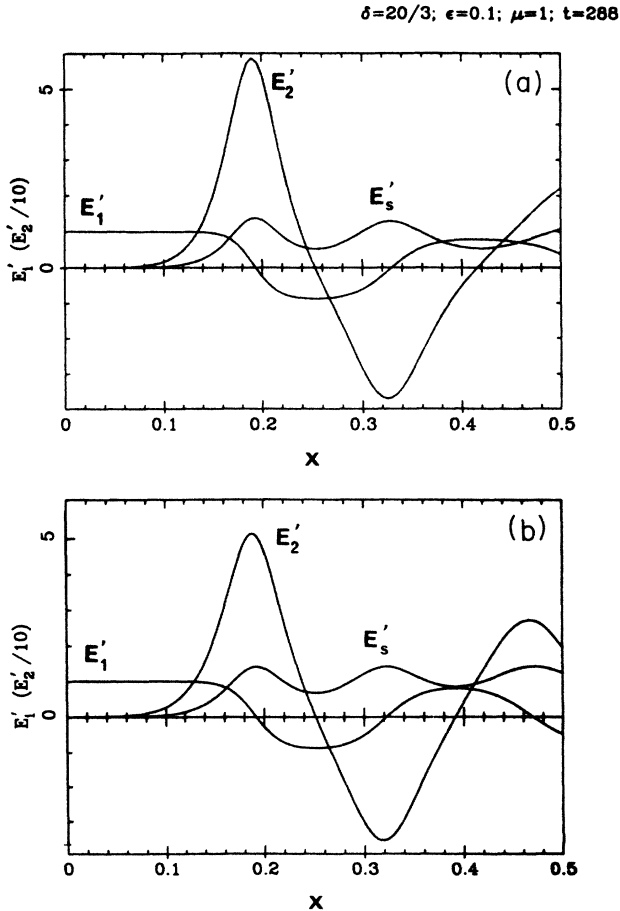


FIG. 7. Same comparison as in Fig. 6 for the case $\mu \neq 0$ ($\mu=1$) for $t=288$. The two graphs (a) and (b) are restricted to the neighborhood of the first peak.

laser power, and a pulse long enough to contain 400 interaction times (an interaction length of 500 m), then we find that $\epsilon_0 E_2^2 \simeq 50$ bars, a value which is not so far from P_f .

At this point a new interesting problem arises. We have seen that important pressure gradients are likely to appear on the fiber as a result of the nonlinear propagation of the backward pulse. Therefore large local constraints have been set up, which will propagate along the fiber after the passage of the e.m. pulse, and we can expect that this propagation itself will exhibit a nonlinear behavior. Nonlinear propagation of a longitudinal strain in an elastic medium is not a usual matter. We have already derived the equation of propagation along a thin rod starting from an expression of the free energy of the elastic medium expanded up to third order in terms of the stress tensor components. Our preliminary results show that the solutions have a characteristic tendency of steepening the initial gradients, which suggests that this nonlinear propagation may be an additional factor reinforcing the initial constraints produced by the radiation pressure. A detailed study of this phenomenon will be presented in a forthcoming paper.

ACKNOWLEDGMENTS

We thank Dr. J. Peyraud, Dr. J. Botineau, Dr. A. Saissy, and Dr. M. Casanova for stimulating discussions. Laboratoire de Physique de la Matière Condensées is Laboratoire No. 190 associé au Centre National de la Recherche Scientifique (France).

APPENDIX A

Let $E_i = \rho_i e^{i\varphi_i}$. With the chosen initial conditions, initial phases φ_1^0 and φ_2^0 are obviously independent of x (φ_1^0 can be taken null) while φ_s^0 is undetermined ($E_s = 0$). The following argument shows that $\varphi_i(x, t)$ keep constant values in time.

First we observe that our initial conditions actually determine φ_s at $t=0_+$. Indeed Eqs. (8) for E_s implies that $\lim_{h \rightarrow 0} E_s(x, h) = h E_1(x, 0) E_2^*(x, 0)$, which gives $\varphi_s(x, 0_+) = -\varphi_2^0$. Let us rewrite Eqs. (8) in terms of the ρ_i and φ_i :

$$\begin{aligned} (\partial_t + \partial_x)\rho_1 &= -\rho_2 \rho_s \cos\varphi, \\ (\partial_t - \partial_x)\rho_2 &= \rho_1 \rho_s \cos\varphi, \end{aligned} \quad (\text{A1})$$

$$\begin{aligned} (\partial_t + \epsilon \partial_x + \mu)\rho_s &= \rho_1 \rho_s \cos\varphi, \\ (\partial_t + \partial_x)\varphi_1 &= (\rho_2 \rho_s / \rho_1) \sin\varphi, \\ (\partial_t - \partial_x)\varphi_2 &= (\rho_1 \rho_s / \rho_2) \sin\varphi, \\ (\partial_t + \epsilon \partial_x)\varphi_s &= (\rho_1 \rho_2 / \rho_s) \sin\varphi, \end{aligned} \quad (\text{A2})$$

where $\varphi = \varphi_1 - (\varphi_2 + \varphi_s)$.

Let us now consider slightly different initial conditions, namely the φ_i 's keep the above values ($\varphi_1^0 = 0$, $\varphi_s^0 = -\varphi_2^0$)

but $\rho_s^0 \neq 0$. Then $\varphi^0 = 0$ and since $\partial_x \varphi_i^0 = 0$, Eqs. (A2) give $\partial_t \varphi_i(x, 0) = 0$. Now it is easily seen that $\partial_t^2 \varphi_i(x, 0)$ also vanish. For instance, we have

$$\partial_t^2 \varphi_1 = -\partial_x \partial_t \varphi_1 + \partial_t (\rho_2 \rho_s / \rho_1) + (\rho_2 \rho_s / \rho_1) (\cos\varphi) \partial_t \varphi,$$

which vanishes at $t=0$. In the same way all the time derivatives of the φ_i 's vanish at $t=0$. Assuming the analyticity of the φ_i 's at initial time we conclude that they reduce to constants. Making now $\rho_s^0 \rightarrow 0$, we obtain our previous initial conditions at $t=0_+$, which ends the proof.

APPENDIX B

It is convenient, for numerical integration, to remove in Eqs. (8), for $\epsilon=0$, the space derivatives by introducing the new functions $z_i(x, t)$ defined by

$$\begin{aligned} z_1(x, t) &= Y_1(x + 2t, t), \\ z_2(x, t) &= Y_2(x, t), \\ z_s(x, t) &= Y_s(x + t, t). \end{aligned}$$

Then the z_i 's obey the following nonlocal equations in x :

$$\begin{aligned} \partial_t z_1(x, t) &= -z_2(x + 2t, t) z_s(x + t, t), \\ \partial_t z_2(x, t) &= z_1(x - 2t, t) z_s(x - t, t), \\ (\partial_t + \mu) z_s(x, t) &= z_1(x - t, t) z_2(x + t, t). \end{aligned}$$

Discretizing variable x by setting $x = jh$, we obtain a set of functions $z_\alpha^j(t)$, obeying ordinary differential equations. These equations will be considered as depending explicitly on time through the spatial arguments of z_α^j functions, namely: $x \pm t$, $x \pm 2t$. We can then apply to the numerical integration of these equations a standard four-step Runge-Kutta algorithm. However we must consider the stability of this algorithm. It is known, in the case of PDE describing counterstreaming wave interaction that a numerical instability occurs when the spatial step h is larger or equal to the temporal step h_0 . We have therefore been led to use $h = h_0/2$. Then at each step of integration the pairwise z_α^j 's are incremented according to the Runge-Kutta algorithm, while the odd ones are calculated by four-term interpolation using the pairwise z_α^j 's. This procedure proves to be remarkably stable.

APPENDIX C

From Eqs. (19) and (20) of the main text, we find that Y_2 obeys the following equation:

$$(\partial_t^2 + \partial_x \partial_t + \mu \partial_t) Y_2 = Y_2, \quad (\text{C1})$$

where we have made the change of variable $x \Rightarrow x/(1 + \epsilon)$. Initial and boundary conditions are

$$\begin{aligned}
 Y_s(x,0) &= 0, \\
 Y_2(x,0) &= \rho x^n \quad (n \text{ integer}), \\
 Y_s(0,t) &= 0.
 \end{aligned}$$

From the two last relations we deduce $\partial_t Y_2(0,t) = Y_2(0,t) = 0$. Taking the Laplace transform of

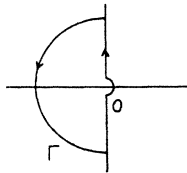
$$y(x,s)/\rho = -x^n/a - (1+a/s) \left[\sum_{k=1}^{n-1} n(n-1)\cdots(n-k+1)x^{n-k}/a^{k+1} + n!(1-e^{ax})/a^{n+1} \right], \tag{C3}$$

with $a = (1 - \mu s - s^2)/s$.

A priori the singularities of $y(x,s)$ in s space are located at $s=0$ and at the roots $s_{1,2}$ of $a=0$. It can be shown that $s_{1,2}$ are not poles of the above expression. Indeed $y(x,s)$ reduce, in the vicinity of $a=0$, to

$$y(x,s)/\rho = x^n/s^2 + n!(1-\mu s)/s^2 \sum_{k=n+1}^{\infty} x^k a^{k-(n+1)}/k!,$$

which expression is regular for $a=0$. We are therefore left with the unique $s=0$ singularity. Inverting the Laplace transformation, we shall use for $t > x$ the following Γ contour in the s -complex plane:



Finally the only contribution to this integral comes from the essential singularity at $s=0$ associated with the exponential term e^{ax} in expression (C3), and we obtain

$$Y_2(x,t)/\rho = n! \int_{\Gamma} (1+a/s)e^{ax}e^{st}/a^{n+1} ds.$$

The residue of $s=0$ singularity is obtained by expanding the integrand in powers of s . In the limit of large t , we obtain

$$Y_2(x,t)/\rho = n! x^n \sum_{k=0}^{\infty} \xi^k / (k!(n+k)!), \tag{C4}$$

where $\xi = xt/(1+\epsilon)$ (returning to old x variable). Expression (C4) can be expressed in terms of a Bessel function of imaginary argument:

$$Y_2(x,t) = \rho n! (i)^{-n} t^{-n} \xi^{n/2} J_n(2i\sqrt{\xi}). \tag{C5}$$

This result can be rederived by looking for an asymptotic solution of Eqs. (19) and (20) of the form $Y_2 = t^\alpha \varphi_2(\xi)$, $Y_s = t^\beta \varphi_s(\xi)$. The argument given in the main text only leads to the relation $\beta = \alpha - 1$, and not to the complete determination of α and β values (this is due to the absence of the equation obeyed by Y_1). We then obtain

$$(1/\varphi_s)(\alpha + \xi d/d\xi)\varphi_2 = (1/\varphi_2)d\varphi_s/d\xi = 1,$$

Eq. (C1) yields

$$[(s^2 - 1) + s(\partial_x + \mu)]y(x,s) = (s + \mu + \partial_x)Y_2(x,0), \tag{C2}$$

where $y(x,s)$ is the Laplace transform of $Y_2(x,t)$.

Integrating Eq. (C2) with respect to variable x , and accounting for the boundary conditions, gives

from which we deduce the equation obeyed by φ_2 :

$$\xi d^2\varphi_2/d\xi^2 + (\alpha + 1)d\varphi_2/d\xi = \varphi_2, \tag{C6}$$

whose solutions vanishing at the origin are of the form

$$\varphi_2 = A \xi^{-\alpha/2} J_{-\alpha}(2i\sqrt{\xi}).$$

At small ξ , φ_2 behaves like $A(i)^{-\alpha} \xi^{-\alpha}/\Gamma(-\alpha)$, where Γ is the gamma function. Therefore a solution Y_2 proportional to ξ^α (a arbitrary real) at the origin is of the form

$$Y_2 = A t^{-\alpha} (i\xi)^\alpha J_\alpha(2i\sqrt{\xi}), \tag{C7}$$

which formula generalizes result (C5) to the case of noninteger n . Using Eq. (20) we obtain

$$Y_s = A t^{-(\alpha+1)} (i\xi)^\alpha [(1-a)J_\alpha(2i\sqrt{\xi}) - 2i\xi J'_\alpha(2i\sqrt{\xi})]. \tag{C8}$$

APPENDIX D

Equation (27) of the main text can be rewritten as $(\xi\theta')' = -\sin\theta$, from which

$$\theta' = -\xi^{-1} \int_0^\xi \sin\theta(\tau) d\tau, \tag{D1}$$

and we want to show that $|\theta'| \rightarrow 0$ when $\xi \rightarrow \infty$. Eq. (D1) gives

$$|\theta'| \leq 1. \tag{D2}$$

Let us first assume that, at large ξ , $\theta(\xi)$ is a monotonic, say growing, function of ξ . Then inequality (D2) shows that, when $\xi \rightarrow \infty$, either $|\theta'| \rightarrow k < 1$ or $|\theta'| \rightarrow 0$. In the last case the theorem is verified, while in the former case $\theta \rightarrow k\xi + \beta(\xi)$, where $|\beta(\xi)| < \xi$. Then, since $\sin\theta = \sin(k\xi)\cos\beta + \cos(k\xi)\sin\beta$, we have

$$\left| \int_0^\xi \sin\theta d\tau \right| < \left| \int_0^\xi \sin(k\xi) \right| + \left| \int_0^\xi \cos(k\xi) \right| < \infty,$$

and by Eq. (D1), $|\theta'| \rightarrow 0$.

Now this argument can be extended to the case where $\theta(\xi)$ is unbounded but no longer monotonic. More precisely we assume that $|\theta| < A(\xi)$, with $A(\xi)$ monotonic, and that $\lambda(\xi) = \theta/A$ is such that $\xi^{-1} \int_0^\xi \lambda(\tau) d\tau \neq 0$ when $\xi \rightarrow \infty$. $\lambda(\xi)$ and A' are bounded. From $\theta' = A'\lambda + A\lambda'$ and Eq. (D2) we conclude that $\lambda' \rightarrow 0$. Since $\xi^{-1} \int_0^\xi \lambda(\tau) d\tau \neq 0$, then $\lambda \rightarrow k \neq 0$. We conclude that $|\theta'| \rightarrow kA$, and we recover the preceding case.

In the last case to be considered, θ will be assumed bounded. We shall show that $|\xi^{-1} \int_0^\xi \sin\theta d\tau|$ either goes to zero or to a finite value k as $\xi \rightarrow \infty$. Let us put $\theta = \rho + \alpha(\xi)$ with $\int_{-\infty}^\infty \alpha d\xi < \infty$. Then $\alpha(\xi)$ has a well-defined Fourier transform: $\alpha(\xi) = \sum_k \alpha_k \cos(k\xi + \mu_k)$. Now $\sin\theta = \sin(\rho + \alpha)$ can be expanded in terms of Bessel functions as

$$\sin\theta \simeq e^{i\rho} \prod_k e^{i\alpha_k \cos(k\xi + \mu_k)} - \text{c.c.},$$

with

$$e^{i\alpha_k \cos(k\xi + \mu_k)} = \sum_n i^n J_n(\alpha_k) e^{in(k\xi + \beta_k)}.$$

Then $\sin\theta$ appears as a sum of terms proportional to $e^{i \sum_i n_i (k_i \xi + \beta_i)}$, whose contribution to expression (D1) vanishes except for terms where $\sum_i n_i (k_i \xi + \beta_i) = 0$, which terms yield a ξ -independent contribution. Finally we obtain that $\theta' \rightarrow B$ (B constant). Therefore $\theta \rightarrow B\xi + \nu(\xi)$, with $|\nu| < \xi$ and putting this asymptotic expression in Eq. (D1) we obtain as above that $|\theta'| \rightarrow 0$.

- ¹D. Cotter, *J. Opt. Commun.* **4**, 10 (1983), and references therein.
²E. P. Ippen and R. H. Stolen, *Appl. Phys. Lett.* **21**, 539 (1972).
³C. Montes, *Phys. Rev. A* **31**, 2366 (1985), and references therein.
⁴N. Kroll, *J. Appl. Phys.* **36**, 34 (1965).
⁵M. Damzen and H. Hutchinson, *IEEE J. Quantum Electron.* **QE-19**, 7 (1983).
⁶I. Bar-Joseph, A. Friesem, E. Lichtman, and R. G. Waarts,

J. Opt. Soc. Am. **2**, 1606 (1985).

⁷F. Chu and C. Karney, *Phys. Fluids* **20**, 1728 (1977).

⁸D. Kaup, A. Reiman, and A. Bers, *Rev. Mod. Phys.* **51**, 275 (1979).

⁹G. L. Lamb, Jr., *Phys. Lett.* **29A**, 507 (1969).

¹⁰G. L. Lamb, Jr., *Rev. Mod. Phys.* **43**, 99 (1971).

¹¹G. Lamb, Jr., *Elements of Soliton Theory* (Wiley, New York, 1980), p. 153.